Author's response to the interactive discussion

Meng Sun (correspondent author)

January 5, 2026

In the following, we will answer each reviewer's comments point-by-point.

1 st reviewer's comments

Comments can be found at https://doi.org/10.5194/egusphere-2025-2671-RC1. These comments are given by italic texts below.

The authors want to express our sincere gratitude to the reviewer for taking the time to review our manuscript. Your thoughtful feedback and constructive suggestions have been immensely valuable in improving the quality of our work.

1.1 Overall assessment

In the first review, I pointed out issues mainly in two aspects: (1) a lack of clarity in the derivation process, and (2) weaknesses in the numerical testing framework, particularly the lack of reliable benchmarks.

Regarding the first aspect, some of the concerns and confusions have been alleviated in the revision. However, other revisions remain rather superficial, and several important concerns regarding the credibility of the derivation largely remain unaddressed. Some of the major comments listed below repeat those from the initial review, as the authors' responses did not fully tackle the core issues.

As for the second aspect, instead of providing additional comparisons with reliable benchmarks, the authors have weakened the tone of their claims on "validation" or "verification." Since the formulation depends on several empirical parameters that are only loosely constrained, the numerical tests do not meaningfully demonstrate the advantage of the new parameterization or provide physical insights.

Given the current quality of the manuscript, its scientific significance does not meet the standard required for publication in Ocean Science.

We apologize for not adequately address the reviewer's core concerns in the first revision of our manuscript. The authors fully agree with the reviewer's suggestion that our manuscript should be edited by native English speakers.

1.2 Major comments

1.2.1 *L9: "provided and validated tentatively"*

The authors slightly modified the wording, but it still seems to overstate the credibility of the results. The presented comparisons with the lake experiment are not robust enough to "validate" the formulation. If the authors intend to emphasize the physical insights gained from the comparison, those points should be stated more clearly.

We removed this sentence and supplemented some objective descriptions, physical insights and model deficiencies as:

> Comparisons of the TKE dissipation rates indicate that the model results agree well with the laboratory observations which were directly generated by the waves themselves, but for mechanical and wind waves, dispersions suggest the presence of other dynamic processes. The modeled attenuation coefficients of the breaking spectrum correspond to the decreasing tendency measured from the lake experiment, which yields valuable insights of the physics of dominant breaking, but the statistical approach is less well-suited for simulating the rapid transient regime of wave breaking as well as for the higher frequency in the equilibrium range.

1.2.2 *L11 and L572: "Numerical results indicate that the wave energy dissipation … is inadequate, … wave-generated turbulence play critical roles of wave energy loss." "… that the wave energy loss only induced by wave-breaking appears to be inadequate, …"*

Since the authors attempt to draw physical interpretations without any quantitative comparison against reliable reference data, the simulation results are not sufficiently credible to identify the relevant physical processes. Therefore, these statements are not supported by the presented evidence, and I would recommend removing them.

We agree with the reviewer's opinion that these arguments lack sufficient experimental validations in the manuscript. And they are a little out of scope for the present study, so we removed these sentences in the revision.

1.2.3 *Eq.(1) and Appendix A:*

The authors added Appendix A, which is very helpful for the readers to grasp the derivation of Eq. (1). Still, some implicit yet important assumptions (which can be only inferred from the derivation) should be made explicit so that the readers can assess the reliability of the formulations:

- *Timescale separation is assumed such that turbulence timescale is much shorter than wave period.*
- *Reynolds stress components are represented with k - ε type eddy viscosity model.*

According to the reviewer's suggestion, we added these assumptions to the text and appendix of the revised manuscript.

1.2.4 *Eq.(12):*

In the first review, I have pointed out Eq. (12) is unsupported by the information provided so far. The authors have rephrased some description, but the problem mostly remains as it was. What did Yuan et al. (2013) proposed, how does l_D come in the formulation, and what does the new choice physically mean?

As per the reviewer's suggestions, we outline the derivation processes of Eq. (12), Eq. (15) and Eq. (19) briefly into Appendix B of the revised manuscript.

Appendix B

Brief derivations of Eq. (12), Eq. (15) and Eq. (19)

Yuan et al. (2013) proposed equilibrium solutions of the k - ε type eddy viscosity model from the minimization relation, and the TKE dissipation rate ε can be expressed as

$$\overline{\varepsilon} \approx \frac{7}{8}\frac{\overline{k}^2}{\pi^2\overline{\varepsilon}}\left(\frac{\partial u_{\mathrm{SM}i}}{\partial x_j}\right)^2 \tag{B1}$$

The approximate coefficient 7/8 indicates that the shear instability generation of surface waves is the dominant source of the turbulence in the upper ocean. Based the mixing length of $\overline{l}_D = \dfrac{\overline{k}^{3/2}}{\pi^{3/2}\overline{\varepsilon}}$ (Baumert et al., 2005), $\overline{k}$, $\overline{\varepsilon}$ are formulated conveniently as

$$\overline{k} = \frac{7}{8}\pi\overline{l}_{\mathrm{D}}^{\,2}\left(\frac{\partial u_{\mathrm{SM}i}}{\partial x_j}\right)^2$$

$$\overline{\varepsilon} = \left(\frac{7}{8}\right)^{3/2}\overline{l}_{\mathrm{D}}^{\,2}\left(\left|\frac{\partial u_{\mathrm{SM}i}}{\partial x_j}\right|\right)^3$$

Then the mixing coefficient $\left\langle \dfrac{\overline{k}^2}{\pi^2\overline{\varepsilon}} \right\rangle_{\mathrm{SM}}$ is expressed as

$$\left\langle \frac{\overline{k}^2}{\pi^2\overline{\varepsilon}} \right\rangle_{\mathrm{SM}} = \left(\frac{7}{8}\right)^{1/2}\left\langle \overline{l}_{\mathrm{D}}^{\,2} \right\rangle_{\mathrm{SM}}\left\langle \left|\frac{\partial u_{\mathrm{SM}i}}{\partial x_j}\right| \right\rangle_{\mathrm{SM}} \tag{B2}$$

Yuan et al. (2013) discussed the relation of the classical Prandtl mixing-length theory (Yuan et al., 1999) with the equilibrium solution of the k - ε type eddy viscosity model by the available 12 groups of field data measurements. Here in this study, only the wave-generated turbulence is considered, so we let

$$\overline{l}_{\mathrm{D}} \approx \left| \iint_{\vec{k}} A\frac{\cosh K(\hat{H}+x_3)}{\sinh K\hat{H}} \exp\left\{ i\left(\vec{\boldsymbol{k}}\cdot\vec{\boldsymbol{r}} - \omega t\right)\right\} \mathrm{d}\vec{\boldsymbol{k}} \right| \tag{B3}$$

where the wavenumber vector $\vec{\boldsymbol{k}} = \left(k_1,\ k_2\right)$ with $K = \sqrt{k_1^2 + k_2^2}$, $\vec{\boldsymbol{r}} = \left(x_1,\ x_2\right)$. ω denotes the radian frequency, and A, the wave amplitude. $\left\langle \overline{l}_{\mathrm{D}}^{\,2} \right\rangle_{\mathrm{SM}}$, $\left\langle \dfrac{\partial u_{\mathrm{SM}i}}{\partial x_j}\dfrac{\partial u_{\mathrm{SM}i}}{\partial x_j} \right\rangle_{\mathrm{SM}}$ can be expressed in wavenumber spectrum as

$$\left\langle \overline{l}_D^{\,2} \right\rangle_{\mathrm{SM}} \approx \iint_{\vec{k}} E(k_1,k_2)\frac{\cosh^2 K(\hat{H}+x_3)}{\sinh^2 K\hat{H}}\mathrm{d}k_1\mathrm{d}k_2$$

$$\left\langle \frac{\partial u_{\mathrm{SM}i}}{\partial x_j}\frac{\partial u_{\mathrm{SM}i}}{\partial x_j}\right\rangle_{\mathrm{SM}} = \iint_{\vec{k}} 2\omega^2 K^2 \frac{\cosh 2K(\hat{H}+x_3)}{\sinh^2 K\hat{H}} E(k_1,k_2)\mathrm{d}k_1\mathrm{d}k_2$$

Then the mixing coefficient is reduced to

$$\left\langle \frac{\bar{k}^2}{\pi^2\bar{\varepsilon}}\right\rangle_{\mathrm{SM}} = \frac{\sqrt{7}}{2}\iint_{\vec{k}} E(k_1,k_2)\frac{\cosh^2 K(\hat{H}+x_3)}{\sinh^2 K\hat{H}}\mathrm{d}k_1\mathrm{d}k_2\left(\iint_{\vec{k}} \omega^2K^2\frac{\cosh 2K(\hat{H}+x_3)}{\sinh^2 K\hat{H}}E(k_1,k_2)\mathrm{d}k_1\mathrm{d}k_2\right)^{1/2} \qquad \text{(B4)}$$

which is Eq. (12) in Section 2.1.

For deep water depth, $\frac{\cosh K(\hat{H}+x_3)}{\sinh K\hat{H}} \sim \exp\{Kx_3\}$, $\frac{\cosh 2K(\hat{H}+x_3)}{\sinh^2 K\hat{H}} \sim 2\exp\{2Kx_3\}$, then Eq. (B4) is reduced to

$$\left\langle \frac{\bar{k}^2}{\pi^2\bar{\varepsilon}}\right\rangle_{\mathrm{SM}} = \sqrt{\frac{7}{2}}\iint_{\vec{k}} E(k_1,k_2)\exp\{2Kx_3\}\mathrm{d}k_1\mathrm{d}k_2\left(\iint_{\vec{k}} \omega^2K^2E(k_1,k_2)\exp\{2Kx_3\}\mathrm{d}k_1\mathrm{d}k_2\right)^{1/2} \qquad \text{(B5)}$$

which is Eq. (13) in Section 2.1.

For future practical applications, we introduce some characteristic wavenumbers and frequencies for various integral mean variables, i.e.,

$\iint_{\vec{k}} E(k_1,k_2)\exp\{2Kx_3\}\mathrm{d}k_1\mathrm{d}k_2 \approx \exp\{2\hat{K}_1x_3\}\iint_{\vec{k}} E(k_1,k_2)\mathrm{d}k_1\mathrm{d}k_2$,

$\iint_{\vec{k}} \omega^2K^2E(k_1,k_2)\exp\{2Kx_3\}\mathrm{d}k_1\mathrm{d}k_2 \approx \hat{\omega}^2\hat{K}_2^2\exp\{2\hat{K}_2x_3\}\iint_{\vec{k}} E(k_1,k_2)\mathrm{d}k_1\mathrm{d}k_2$,

$\iint_{\vec{k}} \frac{1}{2K+2\hat{K}_1+\hat{K}_2}\omega^2K^2E(k_1,k_2)\mathrm{d}k_1\mathrm{d}k_2 \approx \frac{1}{5\hat{K}_3}\iint_{\vec{k}} \omega^2K^2E(k_1,k_2)\mathrm{d}k_1\mathrm{d}k_2$.

Here we assume that $\hat{K}_1 \approx \hat{K}_2 \approx \hat{K}_3 \approx \hat{K}$ approximately. After some algebraic procedures, Eq. (B5) is reduced to

$$\left\langle \frac{\bar{k}^2}{\pi^2\bar{\varepsilon}}\right\rangle_{\mathrm{SM}} \approx \sqrt{\frac{7}{2}}\hat{\omega}\hat{K}\left(\iint_{\vec{k}} E(k_1,k_2)\mathrm{d}k_1\mathrm{d}k_2\right)^{3/2}\exp\{3\hat{K}x_3\} \qquad \text{(B6)}$$

which is Eq. (14) in Section 2.1. And by using the above unified $\hat{\omega}, \hat{K}$ and employing Eq. (B6), Eq. (11) in Section 2.1 can be derived as

$$S_{\mathrm{tid}} \approx -\frac{2\sqrt{14}}{5}\alpha_{\mathrm{wt}}K^3\hat{\omega}\left(\iint_{\vec{k}} E(k_1,k_2)\mathrm{d}k_1\mathrm{d}k_2\right)^{3/2}E(k_1,k_2) \qquad \text{(B7)}$$

which is Eq. (15) in Section 2.1 for our further convenient numerical applications.

For monochromatic non-breaking waves, the derivation processes are similar as above. For deep water depth, we have

$$\left\langle \overline{l}_{\mathrm{D}}^2\right\rangle_{\mathrm{SM}} \approx \frac{1}{2}A^2\exp(2Kx_3) .$$

$$\left\langle \frac{\partial u_{\mathrm{SM}i}}{\partial x_j}\frac{\partial u_{\mathrm{SM}i}}{\partial x_j}\right\rangle_{\mathrm{SM}} = 2A^2\omega^2K^2\exp(2Kx_3) .$$

and

$$\left\langle \frac{\bar{k}^2}{\pi^2 \bar{\varepsilon}} \right\rangle_{\mathrm{SM}} = \frac{\sqrt{7}}{4} A^3 \omega K \exp\{3Kx_3\}$$

.

By employing Eq. (B1), the TKE dissipation rate $\varepsilon_{\mathrm{dis}}$ can be derived as

$$\varepsilon_{\mathrm{dis}} \approx \alpha_{\mathrm{wt}} \frac{7}{8} \left\langle \frac{\bar{k}^2}{\pi^2 \bar{\varepsilon}} \right\rangle_{\mathrm{SM}} \left\langle \left(\frac{\partial u_{\mathrm{SM}\,i}}{\partial x_j} \right)^2 \right\rangle_{\mathrm{SM}} = \frac{7\sqrt{7}}{16} \alpha_{\mathrm{wt}} A^5 \omega^3 K^3 \exp\{5Kx_3\} \tag{B8}$$

which is Eq. (19) in Section 2.1.

1.2.5 *L304-324 and response 2.2.4:*

Original comment, designated as "L286-310", was meant for the experiment series of Wei et al. (2018), described in Table 1, and plotted in Figure 4. They are strongly influenced by wind. Without considering other terms in TKE equation, the comparison between $\varepsilon_{\mathrm{dis}}$ *and* e_{tid} *does not make much sense.*

We agree with the reviewer's point that the TKE production by breaking waves, wind-driven shear turbulence and the Langmuir turbulence are likely significant for the TKE balance. In the laboratory experiments, the measurements were recorded for nonbreaking waves, and the wave steepness in Table 1 is less than the classical breaking criterion 1/7, so the breaking effects can in fact be neglected here. Actually in the ocean, the TKE production can be originated from the wind-driven shear flow. The wave-induced mixing strength is much larger than that calculated from the Mellor-Yamada turbulence closure scheme in the upper layers (e.g. Qiao et al., 2010; Xia, 2015). The latter can also be neglected here in the laboratory experiments, for the wind wave tank is only 16 m long and the near-surface wind-driven turbulence is still in its incipient stage due to the short fetch. There are a number of studies about the interaction of ocean waves with upper ocean turbulence induced by Stokes drift shears, which accounts for a significant fraction of the energy losses of the wave field (e.g. McWilliams et al., 1997; Teixeira and Belcher, 2002; Ardhuin and Jenkins, 2006). Teixeira & Belcher (2002) studied distortion of turbulence by Stokes drift and evaluated the corresponding wave energy loss induced by Langmuir turbulence, which is approximately a factor of 3 smaller than the amplitude growth rate due to forcing by the wind, through a complemented linear RDT model. McWilliams et al. (2000) investigated the vertical mixing induced by Langmuir turbulence through an improved K-profile parameterization (KPP). In the following, we estimate roughly the TKE dissipation rates of Langmuir turbulence by using the classical Prandtl mixing-length theory,

$$\langle \bar{\varepsilon} \rangle_{\mathrm{SM}} \approx \left\langle \bar{l}_{\mathrm{D}}^2 \right\rangle_{\mathrm{SM}} \left\langle \left(\left| \frac{\partial U_{\mathrm{S}}}{\partial x_3} \right| \right)^3 \right\rangle_{\mathrm{SM}} = \frac{1}{2} A^2 \exp\{2Kx_3\} \cdot \left\{ 2\omega K^2 A^2 \exp\{2Kx_3\} \right\}^3 = 4\omega^3 K^6 A^8 \exp\{8Kx_3\}$$

where the Stokes drift is $U_{\mathrm{S}} = \omega K A^2 \exp\{2Kx_3\}$ (Mcwilliams et al., 1997). The following figure shows the dependence of TKE dissipation rate of Langmuir turbulence versus layer depth in linear/logarithmic scale for various wave conditions respectively. For case 4 in Table 1, the estimated TKE dissipation rates are less than 10^{-6} m^2 s^{-3}, which are not shown in the figure. Comparison with Figure 4 in Section 2.1 indicates the TKE dissipation rates of Langmuir

turbulence are 1-2 orders of magnitude smaller than those from our model. Since these results are beyond the scope of the paper, we do not add them to the text.

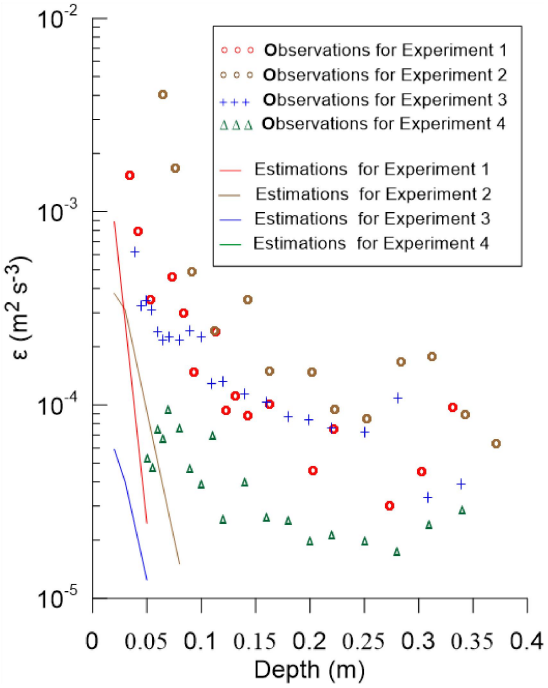

Figure A1. Dependence of TKE dissipation rate $\varepsilon_{\mathrm{dis}}$ (denoted as ε in the figure) versus layer depth. Observation data (circles, pluses and triangles) are digitalized from Wei et al. (2018). The estimations of the TKE dissipation rate of Langmuir turbulence are shown with solid lines. Data are plotted in linear/logarithmic scale on the horizontal/vertical axis.

Key references

Qiao, F., Yuan, Y., Ezer, T., Xia, C., Yang, Y., Lv, X., and Song, Z.: A three-dimensional surface wave–ocean circulation coupled model and its initial testing, Ocean Dyn., 60(5), 1339-1355, https://doi.org/10.1007/s10236-010-0326-y, 2010.

Xia, C. (Eds.): The establishment of the wave-current coupled model based on POM and its applications in the ocean and the coastal sea (in Chinese), China Ocean Press, Beijing, China, 90pp., ISBN 978-7-5027-9258-9, 2015.

Teixeira, M. A. C., and Belcher S. E.: On the distortion of turbulence by a progressive surface wave. J. Fluid Mech., 458, 229-267, 2002.

McWilliams, J. C., Sullivan P. P., and Moeng C.-H.: Langmuir turbulence in the ocean. J. Fluid Mech., 334, 1-30, 1997.

McWilliams, J. C., and P. P. Sullivan: Vertical mixing by Langmuir circulations. Spill Sci. Technol. Bull., 6, 225-237, 2000.

Ardhuin, F., and Jenkins, A. D.: On the interaction of surface waves and upper ocean turbulence, J. Phys. Oceanogr., 36, 551-557, https://doi.org/10.1175/JPO2862.1 , 2006.

1.2.6 *Eq. (26):*

The derivation of Eq. (26) still lacks clear logical steps connecting Eq. (21) or (24) to it. Although the authors have reinforced the description of the underlying physical assumptions, it remains unclear how the formula can be transformed into this form. Therefore, the fundamental questions raised in the previous review remain unaddressed.

We apologize for the fact that this portion of the argument is excessively descriptive and lacks logical derivations. As per the reviewer's suggestions, we outline the derivation processes of Eqs. (24-27) briefly into Appendix C of the revised manuscript.

Appendix C

Brief derivations of Eqs. (24-27)

Assuming that the surface elevation is Gaussian and stationary and breaking occurs wherever the vertical acceleration of the surface exceeds the dynamic criterion (Longuet-Higgins, 1969; Yuan et al., 1986), the surface limited by breaking can be expressed by the Heaviside unit step function, and the postbreaking wave spectrum, via the complicated 0-1st order asymptotic expansions of the Fourier-domain covariance of surface elevation, can be formulated as Eq. (24) in Section 2.2 (Yuan et al., 1986; Hua and Yuan, 1992; Yuan et al., 1993):

$$\alpha_{\mathrm{b}} = \left[1 - 4(2\pi)^{-1/2} \frac{\rho\omega^2 \mu_0^{1/2}}{g} \exp\left(-\frac{\rho^2}{8} \frac{g^2}{\mu_0 \omega_{\mathrm{z}}^4}\right) \right]^2 \tag{C1}$$

where $\omega_{\mathrm{z}} = \left(\frac{\mu_2}{\mu_0}\right)^{1/2}$ denotes the mean zero-crossing wave frequency. Eq. (C1) can be expressed as

$$\alpha_{\mathrm{b}} = 1 - 8(2\pi)^{-1/2} \frac{\rho\omega^2 \mu_0^{1/2}}{g} \exp\left(-\frac{\rho^2}{8} \frac{g^2}{\mu_0 \omega_{\mathrm{z}}^4}\right) + \left[4(2\pi)^{-1/2} \frac{\rho\omega^2 \mu_0^{1/2}}{g} \exp\left(-\frac{\rho^2}{8} \frac{g^2}{\mu_0 \omega_{\mathrm{z}}^4}\right) \right]^2 \tag{C2}$$

The third term on the right-hand side is a higher-order term compared to the second term, because the ratio of the two $r \sim \frac{\rho\omega^2 \mu_0^{1/2}}{g} \sim \rho K \mu_0^{1/2} \sim \rho(AK)$, where $\rho^2 = 1 - \varepsilon_{\mathrm{sp}}^2$, $\varepsilon_{\mathrm{sp}}$ denotes the spectrum width parameter and (AK) denotes the wave steepness. Then the third term is negligible, so the ratio of total energy loss due to wave-breaking is given by

$$r_{\mathrm{b}} = \frac{\iint_{\vec{k}} E(k_1, k_2)\mathrm{d}k_1\mathrm{d}k_2 - \iint_{\vec{k}} E_b(k_1, k_2)\mathrm{d}k_1\mathrm{d}k_2}{\iint_{\vec{k}} E(k_1, k_2)\mathrm{d}k_1\mathrm{d}k_2} \approx 8(2\pi)^{-1/2} \frac{\rho\bar{\omega}^2 \mu_0^{1/2}}{g} \exp\left(-\frac{\rho^2}{8} \frac{g^2}{\mu_0 \omega_{\mathrm{z}}^4}\right) \tag{C3}$$

which is Eq. (25) in Section 2.2.

Yuan et al. (2009) incorporated the breaking surface elevation and the breaking criterion, then derived the breaking kinetic and potential energy loss which add up to deduce the breaking mechanical energy loss. The mechanical energy loss per unit time per unit sea surface area is formulated as

$$E_t = \frac{\rho_0 g \mu_0 \mu_4^{1/2}}{2\pi \mu_2^{1/2}} \rho^2 \left[L \int_{-\infty}^{-L} \exp\left\{-\frac{1}{2}Z^2\right\} dZ + \exp\left\{-\frac{\rho^2}{8} \frac{g^2}{\mu_0 \omega_{\mathrm{z}}^4}\right\} \right] \tag{C4}$$

(Here a slight correction is made to remove the coefficient $\sqrt{2}$ in the denominator in Eq. (54) of Yuan et al. (2009), this minor issue was introduced inadvertently in their Eq. (39) in which the coefficient 4 in the denominator is to be replaced with $2\sqrt{2}$.) Considering the appropriate time scale $T_{\mathrm{b}} = 2\pi(\frac{\mu_2}{\mu_4})^{1/2}$ associated with the loss of energy by wave breaking (Yuan et al., 1993; Donelan and Yuan ,1994), the mechanical energy loss per unit sea surface area is given by

$$\tilde{E} = T_{\mathrm{b}} E_t = \rho_0 g \mu_0 \rho^2 \left[L \int_{-\infty}^{-L} \exp\left\{-\frac{1}{2}Z^2\right\} dZ + \exp\left\{-\frac{\rho^2}{8}\frac{g^2}{\mu_0 \omega_{\mathrm{z}}^4}\right\}\right] \tag{C5}$$

In the neighborhood of wave crests $\mu_0 \bar{\omega}^2 \sim \frac{1}{2}c_0^2$, where $\bar{\omega}$ is the mean wave frequency, c_0 is the characteristic wave speed with $c_0^2 = g^2 \frac{\mu_0^{1/2}}{\mu_4^{1/2}}\rho$ (Yuan et al., 2009), so $\frac{\bar{\omega}^2 \mu_0^{1/2}}{g} = \frac{\bar{\omega}^2 \mu_0}{g\mu_0^{1/2}} \sim \frac{c_0^2}{2g\mu_0^{1/2}} = \frac{g\mu_2}{2\mu_0^{1/2}\mu_4}$. Then

$$\begin{aligned}
\tilde{E} &= \rho_0 g \mu_0 \frac{\mu_2}{\mu_0^{1/2}\mu_4^{1/2}} \rho \left[L \int_{-\infty}^{-L} \exp\left\{-\frac{1}{2}Z^2\right\} dZ + \exp\left\{-\frac{\rho^2}{8}\frac{g^2}{\mu_0\omega_{\mathrm{z}}^4}\right\}\right] \\
&= \rho_0 g \mu_0 \frac{g\mu_2}{2\mu_0^{1/2}\mu_4} \rho \frac{\mu_4^{1/2}}{g/2} \left[L \int_{-\infty}^{-L} \exp\left\{-\frac{1}{2}Z^2\right\} dZ + \exp\left\{-\frac{\rho^2}{8}\frac{g^2}{\mu_0\omega_{\mathrm{z}}^4}\right\}\right] \\
&= \rho_0 g \mu_0 \frac{g\mu_2}{2\mu_0^{1/2}\mu_4} \rho \frac{1}{L} \left[L \int_{-\infty}^{-L} \exp\left\{-\frac{1}{2}Z^2\right\} dZ + \mathrm{e}\exp\left\{-\frac{\rho^2}{8}\frac{g^2}{\mu_0\omega_{\mathrm{z}}^4}\right\}\right] \\
&\sim \rho_0 g \iint_{\vec{k}} \frac{\bar{\omega}^2 \mu_0^{1/2}}{g} \rho \frac{1}{L} \left[L \int_{-\infty}^{-L} \exp\left\{-\frac{1}{2}Z^2\right\} dZ + \exp\left\{-\frac{\rho^2}{8}\frac{g^2}{\mu_0\omega_{\mathrm{z}}^4}\right\}\right] E(k_1,k_2)\mathrm{d}k_1\mathrm{d}k_2 \\
&\sim \rho_0 g \iint_{\vec{k}} \frac{\omega^2 \mu_0^{1/2}}{g} \rho \frac{1}{L} \left[L \int_{-\infty}^{-L} \exp\left\{-\frac{1}{2}Z^2\right\} dZ + \exp\left\{-\frac{\rho^2}{8}\frac{g^2}{\mu_0\omega_{\mathrm{z}}^4}\right\}\right] E(k_1,k_2)\mathrm{d}k_1\mathrm{d}k_2
\end{aligned} \tag{C6}$$

In the final step of the above manipulations, for the spectral wave fields, the mean wave frequency $\bar{\omega}$ should be replaced by ω to depict the localized wave breaking. Then the attenuation coefficient in the wavenumber space is formulated as:

$$\alpha_{\mathrm{b}}' = 1 - \rho \frac{\omega^2 \mu_0^{1/2}}{g} \frac{1}{L} \left[L \int_{-\infty}^{-L} \exp\left\{-\frac{1}{2}Z^2\right\} dZ + \exp\left\{-\frac{\rho^2}{8}\frac{g^2}{\mu_0\omega_{\mathrm{z}}^4}\right\}\right] \tag{C7}$$

which is Eq. (26) in Section 2.2.

Let $\theta \equiv L \int_{-\infty}^{-L} \exp\left\{-\frac{1}{2}Z^2\right\} \mathrm{d}Z \Big/ \exp\left\{-\frac{\rho^2}{8}\frac{g^2}{\mu_0\omega_{\mathrm{z}}^4}\right\}$ represents the ratio of the kinetic energy loss to the potential one due to wave-breaking with a range of 3 to 30 (Yuan et al., 2009; Wang et al., 2017, 2018), Eq. (C7) can be rewritten as

$$\alpha_{\mathrm{b}}' = 1 - \rho \frac{\omega^2 \mu_0^{1/2}}{g} \frac{1+\theta}{L} \exp\left\{-\frac{\rho^2}{8}\frac{g^2}{\mu_0\omega_{\mathrm{z}}^4}\right\} \tag{C8}$$

which is Eq. (27) in Section 2.2.

Key references

Longuet-Higgins, M. S.: On wave breaking and equilibrium spectrum of wind, Proc. Roy. Soc. London, 310A, 151-159, 1969.

Yuan, Y., Tung, C. C., and Huang, N. E.: Statistical characteristics of breaking waves, in: Wave Dynamics and Radio Probing of the Ocean Surface, edited by: Phillips, O. M., and Hasselmann, K., Plenum Press, New York, 265-272, ISBN 0-306-41992-0, 1986.

Hua F., and Yuan, Y.: Theoretical study of breaking wave spectrum and its application, Sci. China Ser. B, 9, 958-965, 1992.

Yuan, Y., Hua, F., Pan, Z., and Sun, L.: Dissipation source function and improvement of LAGFD-WAM numerical wave model, Oceanol. Limnol. Sin., 24(4), 367-376, 1993.

Yuan, Y., Han, L., Hua, F., Zhang, S., Qiao, F., Yang, Y., and Xia, C.: The statistical theory of breaking entrainment depth and surface whitecap coverage of real sea waves, J. Phys. Oceanogr., 39, 143-161, https://doi.org/10.1175/2008JPO3944.1, 2009.

Wang, H., Yang, Y., Sun, B., and Shi, Y.: Improvements to the statistical theoretical model for wave breaking based on the ratio of breaking wave kinetic and potential energy, Sci. China Earth Sci., 60(1), 180-187, https://doi.org/10.1007/s11430-016-0053-3, 2017.

Wang, H., Yang, Y., Dong, C., Su, T., Sun, B., and Zou, B.: Validation of an improved statistical theory for sea surface whitecap coverage using satellite remote sensing data, Sensors, 18, 3306, https://doi.org/10.3390/s18103306, 2018.

1.3 Specific comments and minor issues

1.3.1 *L6 and other parts: "… (turbulence model) with high certainty closure assumptions" The phrase "high certainty closure assumptions" is unusual and potentially misleading, so I would recommend rephrasing it.*

As pointed out in comment 3, the present derivation essentially assumes eddy viscosity formulation to model the Reynolds stress acting on wave orbital motions, which is a nontrivial assumption. In fact, wave-resolving numerical studies show that the Reynolds stress does not vary in phase with the strain rate. (e.g., Guo & Shen, 2014. J. Fluid Mech., 744, 250-272.)

The term "high certainty" introduced by Yuan et al. (2013) was adapted from Baumert's literatures (Baumert and Peters, 2000; Baumert et al., 2005), where they use the term "structural equilibrium". We agree the reviewer's suggestion and rephrased it as "the well-founded structural equilibrium closure assumptions" in the revised manuscript.

We have examined the series of studies of Guo and Shen (2013, 2014), which involves other

dissipation mechanisms and are beyond the scope of our present study. We cited their literatures in the introduction of other dissipation mechanisms in Section 1.

Key references

Baumert, H., and Peters, H.: Second-moment closures and length scales for weakly stratified turbulent shear flows, J. Geophys. Res.,105 (C3), 6453-6468, 2000.

Baumert, H. Z., Simpson, J. H., and Sündermann, J. (Eds.): Marine turbulence: theories, observations, and models, Cambridge University Press, Cambridge, UK, 630pp., ISBN 978-0-521-15372-0, 2005.

Yuan, Y., Qiao, F., Yin, X., and Han, L.: Analytical estimation of mixing coefficient induced by surface wave-generated turbulence based on the equilibrium solution of the second-order turbulence closure model, Sci. China Earth Sci., 56, 71-80, https://doi.org/10.1007/s11430-012-4517-x , 2013.

Guo, X., and Shen, L.: Numerical study of the effect of surface waves on turbulence underneath. Part 1. Mean flow and turbulence vorticity, J. Fluid Mech., 733, 558-587, 2013.

Guo, X., and Shen, L.: Numerical study of the effect of surface waves on turbulence underneath. Part 2. Eulerian and Lagrangian properties of turbulence kinetic energy, J. Fluid Mech., 744, 250-272, 2014.

1.3.2 *Fig. 1:*

How is τ_w *related to the estimation of the growth rate? The figures appear to show smaller wave growth rates when the wave-coherent stress is larger, which seems counterintuitive. Please clarify how these quantities are related.*

The growth rate is dependent on the Miles parameter $\beta = \frac{1.2}{\kappa^2}\mu \ln^4 \mu$ (μ is the dimensionless critical height) and the friction velocity u_*, and the latter two parameters are related to the wave-induced stress τ_w. Janssen (1991) proposed early the quasi-linear growth parameterization for wind input source function S_{in} based on Mile's resonance mechanism, and widely applied in various WAM-Cycle models. To simplify, the wave-induced stress tunes the dimensionless critical height, resulting in a decrease of the Miles parameter via the ratio $\frac{\tau_w}{\tau}$ especially in the high sea state scenario, the figure below roughly shows the dependence of the growth rate $\frac{\gamma}{\omega}$ versus the ratio $\frac{\tau_w}{\tau}$ for a fixed u_*=2.0 m s^{-1} (The effect of wave-induced stress on the drag coefficient is not considered here). And consequently, there is hardly any coupling for old wind sea and the growth rate is dependent on wave age (Janssen, 1991). Figure 1a-c in Section 2.1 exhibits this feature, and Figure 1c corresponds to the severe sea state scenario with old waves or developed waves.

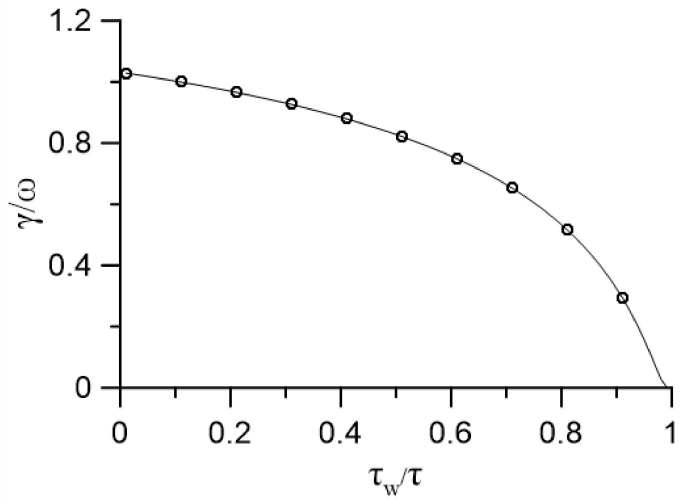

Figure A2. Dependence of the growth rate $\frac{\gamma}{\omega}$ versus the ratio $\frac{\tau_w}{\tau}$ for a fixed u_*=2.0 m s^{-1}.

1.3.3 *Fig. 1 and 2:*

While various combinations of friction velocity and orbital velocity are possible, I would recommend the authors to indicate a realistic comparison. For example, a bulk formula for wind stress and the fetch law (or its limiting form for fully developed sea) would provide a typical relationship between γ *and* γ_{tid}. *Alternatively, authors can provide the estimate of* γ *and* γ_{tid} *from observational data of wind and waves.*

We agree with the reviewer's point that these figures roughly show the scales between the growth and dissipation rates. And we thank the reviewer's suggestion for the realistic comparison, in fact, we are conducting such numerical experiments involving the scaling behavior for the wind input and dissipation source functions. The following figures show side-by-side comparisons in the fetch-limited and duration-limited conditions for steady wind velocity W=15m/s. Since this is not the main topics of the present study, these results and their underlying relationship exploration will be part of our future series papers.

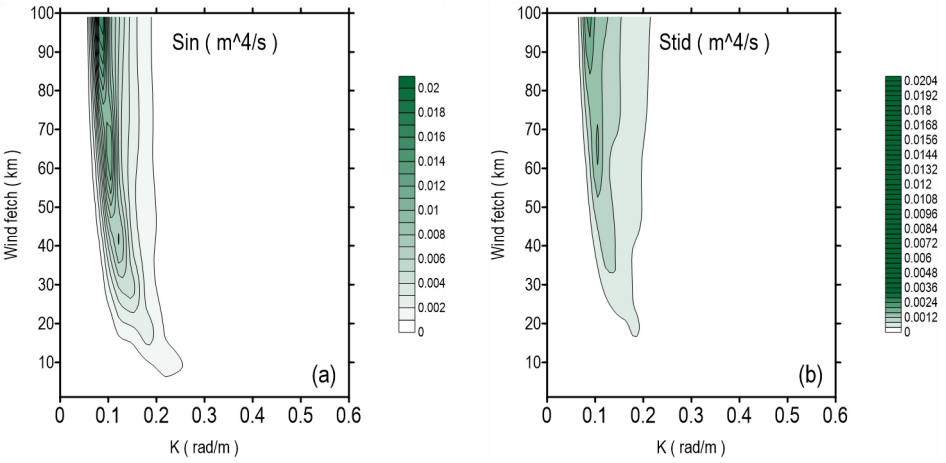

Figure A3. Comparisons between the calculated downwind input term S_{in} (a) and dissipation term

S_{tid} (b) in the fetch-limited conditions for fully developed sea.

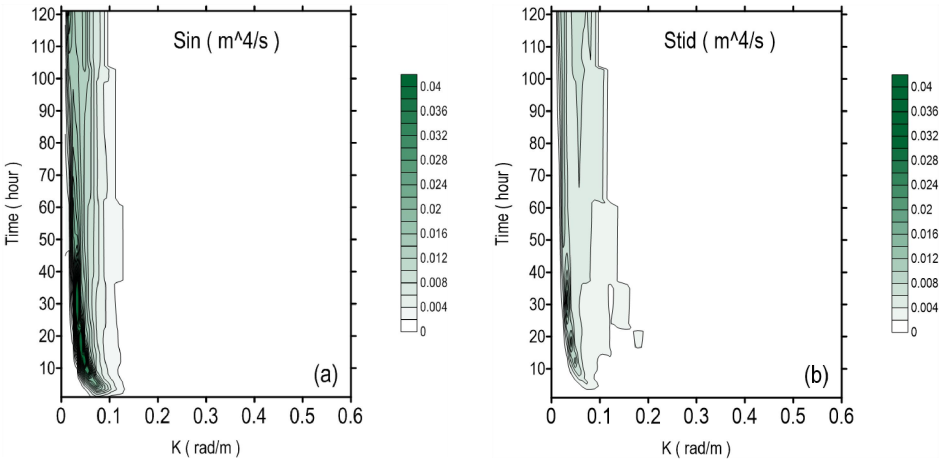

Figure A4. Comparisons between the calculated downwind input term S_{in} (a) and dissipation term S_{tid} (b) in the duration-limited conditions.

1.3.4 *L204 and Response 2.2.12:*

Indeed, those familiar with Fourier transform theory would understand what is intended, but there is no reason to leave such an evidently incorrect and easily correctable expression unchanged. At least in the copy of the Kinsman's textbook at my hand, his use is correct.

L204 should be $\left\langle AA^{*}\exp\left\{i\left[(k_{\alpha}-k'_{\alpha})x_{\alpha}-(\omega-\omega')t\right]\right\}\right\rangle=\delta(\vec{k}-\vec{k}')E(k_1,k_2)$ *and the first and second line of Eq.(7) should be modified correspondingly.*

We apologize for misunderstanding the reviewer's original point. We have now revised Eq. (7) and its preceding paragraph as follows

For a spatially homogeneous and temporally stationary wave field, the product $\left\langle \frac{\partial u_{\mathrm{SM1}}}{\partial x_1}\frac{\partial u_{\mathrm{SM1}}}{\partial x_1}\right\rangle_{\mathrm{SM}}$ is simplified as

$$\begin{aligned}\left\langle \frac{\partial u_{\mathrm{SM1}}}{\partial x_1}\frac{\partial u_{\mathrm{SM1}}}{\partial x_1}\right\rangle_{\mathrm{SM}} &= \iint_{\vec{k}}\mathrm{Re}\left\{\begin{array}{l}\iint_{\vec{k}'}\omega\omega'\dfrac{k_1^2}{K}\dfrac{k_1'^2}{K'}\dfrac{\cosh K(\hat{H}+x_3)}{\sinh K\hat{H}}\dfrac{\cosh K'(\hat{H}+x_3)}{\sinh K'\hat{H}}\\ \left\langle AA^{*}\exp\left\{i\left[(k_{\alpha}-k'_{\alpha})x_{\alpha}-(\omega-\omega')t\right]\right\}\right\rangle\end{array}\right\}\mathrm{d}k_1\mathrm{d}k_2\\ &= \iint_{\vec{k}}\mathrm{Re}\left\{\begin{array}{l}\iint_{\vec{k}'}\omega\omega'\dfrac{k_1^2}{K}\dfrac{k_1'^2}{K'}\dfrac{\cosh K(\hat{H}+x_3)}{\sinh K\hat{H}}\dfrac{\cosh K'(\hat{H}+x_3)}{\sinh K'\hat{H}}\\ \delta(\vec{k}-\vec{k}')E(k_1,k_2)\mathrm{d}k_1'\mathrm{d}k_2'\end{array}\right\}\mathrm{d}k_1\mathrm{d}k_2 \qquad (7)\\ &= \iint_{\vec{k}}\omega^2\frac{k_1^4}{K^2}\frac{\cosh^2 K(\hat{H}+x_3)}{\sinh^2 K\hat{H}}E(k_1,k_2)\mathrm{d}k_1\mathrm{d}k_2\end{aligned}$$

where $\delta(\cdot)$ denotes the Dirac function and $E(k_1,k_2)$, the wavenumber spectrum (Kinsman, 2012).

3 rd reviewer's comments

Comments can be found at https://doi.org/10.5194/egusphere-2025-2671-RC3. These comments are given by italic texts below.

The authors want to express our sincere gratitude to the reviewer for taking the time to review our manuscript. Your thoughtful feedback and constructive suggestions have been immensely valuable in improving the quality of our work.

3.1 Summary

This manuscript presents a theoretical and semi-empirical framework for quantifying turbulent energy dissipation generated by both non-breaking and breaking surface waves. Starting from a unit-volume energy balance, the authors apply a mixing-coefficient turbulence closure in conjunction with linear wave kinematics to derive expressions for wave-generated dissipation in spectral space. The framework is further simplified for deep-water conditions, yielding practical parameterizations (Eqs. 12 to 15) that are suitable for implementation in spectral wave models.

A compact monochromatic formula (Eq. 19) is derived and validated against laboratory measurements, demonstrating that the proposed dissipation model accurately captures the observed dependence on wave amplitude and wavenumber. The framework is further extended to address wave breaking by constructing a statistical post-breaking spectrum and deriving an attenuation coefficient (α_b) based on probabilistic considerations (Eq. 27).

Overall, the authors seek to offer a more physically grounded description of both non-breaking and breaking wave dissipation compared to existing empirical formulations.

The authors thank the reviewer for the overall very comprehensive summary of our work, especially highlighting the main topics of the paper, i.e., the analytical dissipation source functions induced by wave-generated turbulence and wave-breaking, and their validations by comparing to the independent laboratory or in-lake site measurements.

3.2 General Assessment

The manuscript addresses a significant problem: the role of wave-induced turbulence in ocean mixing and in shaping the dissipation source terms used in spectral wave models. Both need more exploration. The attempt to unify non-breaking turbulent dissipation with breaking-wave attenuation within a single theoretical framework is ambitious and scientifically valuable.

The work is conceptually strong, and the physical motivation is clear. However, significant revisions are needed to improve the manuscript's structure, primarily in terms of transparency of derivation, justification of parameters, and clarity of exposition. Some modeling steps are only briefly explained, and several constants appear without sufficient context. Furthermore, the organization occasionally obscures the main logic. The manuscript

would benefit from editing by a native English speaker, as several sentences are unclear in their current form.

Overall, the manuscript contains potentially impactful contributions to the modeling community, but requires major revision to achieve the clarity and rigor expected for publication.

The authors fully agree with the reviewer's suggestion that our manuscript should be edited by native English speakers. As per the reviewer's suggestions, we have revised the manuscript, rephrased and/or extended to improve the text. We hope our supplementary revisions have addressed the reviewer's comments.

3.3 Major Comments

3.3.1 *Need for clearer derivation structure*

Several derivations jump directly from general expressions to reduced forms without showing intermediate steps. This makes it difficult for readers to follow the mathematical logic or reproduce the results. This includes: The reduction steps leading to Eq. 15, which is central to practical modeling; the derivation of the monochromatic dissipation relation (Eq. 19); and the construction of the post-breaking spectrum and attenuation coefficient (Eqs. 24–27). Maybe this could be added in the appendix.

I believe a more explicit presentation of intermediate steps, or a detailed supplementary derivation, would significantly strengthen the work.

We thank the reviewer's suggestions. The reduction steps leading to Eq. (15) and Eq. (19) were supplemented in Appendix B of the revised manuscript (see below). And the constructions of the post-breaking spectrum and attenuation coefficient (Eqs. (24–27)) were supplemented in Appendix C of the revised manuscript (see below).

Appendix B

Brief derivations of Eq. (12), Eq. (15) and Eq. (19)

Yuan et al. (2013) proposed equilibrium solutions of the k - ε type eddy viscosity model from the minimization relation, and the TKE dissipation rate ε can be expressed as

$$\overline{\varepsilon} \approx \frac{7}{8}\frac{\overline{k}^2}{\pi^2 \overline{\varepsilon}}\left(\frac{\partial u_{\mathrm{SM}i}}{\partial x_j}\right)^2 \tag{B1}$$

The approximate coefficient 7/8 indicates that the shear instability generation of surface waves is the dominant source of the turbulence in the upper ocean. Based the mixing length of $\bar{l}_D = \dfrac{\bar{k}^{3/2}}{\pi^{3/2}\bar{\varepsilon}}$ (Baumert et al., 2005), $\bar{k}$, $\bar{\varepsilon}$ are formulated conveniently as

$$\bar{k} = \frac{7}{8}\pi \bar{l}_{\mathrm{D}}^{\,2}\left(\frac{\partial u_{\mathrm{SM}i}}{\partial x_j}\right)^2$$

$$\bar{\varepsilon} = \left(\frac{7}{8}\right)^{3/2} \bar{l}_{\mathrm{D}}^{\,2}\left(\left|\frac{\partial u_{\mathrm{SM}i}}{\partial x_j}\right|\right)^3$$

Then the mixing coefficient $\left\langle \dfrac{\bar{k}^2}{\pi^2\bar{\varepsilon}} \right\rangle_{\mathrm{SM}}$ is expressed as

$$\left\langle \frac{\bar{k}^2}{\pi^2\bar{\varepsilon}} \right\rangle_{\mathrm{SM}} = \left(\frac{7}{8}\right)^{1/2} \left\langle \bar{l}_{\mathrm{D}}^{\,2} \right\rangle_{\mathrm{SM}} \left\langle \left|\frac{\partial u_{\mathrm{SM}i}}{\partial x_j}\right| \right\rangle_{\mathrm{SM}} \tag{B2}$$

Yuan et al. (2013) discussed the relation of the classical Prandtl mixing-length theory (Yuan et al., 1999) with the equilibrium solution of the k - ε type eddy viscosity model by the available 12 groups of field data measurements. Here in this study, only the wave-generated turbulence is considered, so we let

$$\bar{l}_{\mathrm{D}} \approx \left| \iint_{\vec{k}} A \frac{\cosh K(\hat{H}+x_3)}{\sinh K\hat{H}} \exp\left\{ i\left(\vec{\boldsymbol{k}}\cdot\vec{\boldsymbol{r}} - \omega t\right)\right\} \mathrm{d}\vec{\boldsymbol{k}} \right| \tag{B3}$$

where the wavenumber vector $\vec{\boldsymbol{k}} = \left(k_1,\ k_2\right)$ with $K = \sqrt{k_1^2 + k_2^2}$, $\vec{\boldsymbol{r}} = \left(x_1,\ x_2\right)$. ω denotes the radian frequency, and A, the wave amplitude. $\left\langle \bar{l}_{\mathrm{D}}^{\,2} \right\rangle_{\mathrm{SM}}$, $\left\langle \dfrac{\partial u_{\mathrm{SM}i}}{\partial x_j}\dfrac{\partial u_{\mathrm{SM}i}}{\partial x_j} \right\rangle_{\mathrm{SM}}$ can be expressed in wavenumber spectrum as

$$\left\langle \bar{l}_D^{\,2} \right\rangle_{\mathrm{SM}} \approx \iint_{\vec{k}} E(k_1,k_2) \frac{\cosh^2 K(\hat{H}+x_3)}{\sinh^2 K\hat{H}} \mathrm{d}k_1\mathrm{d}k_2$$

$$\left\langle \frac{\partial u_{\mathrm{SM}i}}{\partial x_j}\frac{\partial u_{\mathrm{SM}i}}{\partial x_j} \right\rangle_{\mathrm{SM}} = \iint_{\vec{k}} 2\omega^2K^2 \frac{\cosh 2K(\hat{H}+x_3)}{\sinh^2 K\hat{H}} E(k_1,k_2)\mathrm{d}k_1\mathrm{d}k_2$$

Then the mixing coefficient is reduced to

$$\left\langle \frac{\bar{k}^2}{\pi^2\bar{\varepsilon}} \right\rangle_{\mathrm{SM}} = \frac{\sqrt{7}}{2} \iint_{\vec{k}} E(k_1,k_2) \frac{\cosh^2 K(\hat{H}+x_3)}{\sinh^2 K\hat{H}} \mathrm{d}k_1\mathrm{d}k_2 \left(\iint_{\vec{k}} \omega^2K^2 \frac{\cosh 2K(\hat{H}+x_3)}{\sinh^2 K\hat{H}} E(k_1,k_2)\mathrm{d}k_1\mathrm{d}k_2 \right)^{1/2} \tag{B4}$$

which is Eq. (12) in Section 2.1.

For deep water depth, $\frac{\cosh K(\hat{H}+x_3)}{\sinh K\hat{H}} \sim \exp\{Kx_3\}$, $\frac{\cosh 2K(\hat{H}+x_3)}{\sinh^2 K\hat{H}} \sim 2\exp\{2Kx_3\}$, then Eq. (B4) is reduced to

$$\left\langle \frac{\overline{k}^2}{\pi^2\overline{\varepsilon}} \right\rangle_{\mathrm{SM}} = \sqrt{\frac{7}{2}} \iint_{\vec{k}} E(k_1,k_2)\exp\{2Kx_3\}\mathrm{d}k_1\mathrm{d}k_2 \left(\iint_{\vec{k}} \omega^2 K^2 E(k_1,k_2)\exp\{2Kx_3\}\mathrm{d}k_1\mathrm{d}k_2 \right)^{1/2} \tag{B5}$$

which is Eq. (13) in Section 2.1.

For future practical applications, we introduce some characteristic wavenumbers and frequencies for various integral mean variables, i.e.,

$$\iint_{\vec{k}} E(k_1,k_2)\exp\{2Kx_3\}\mathrm{d}k_1\mathrm{d}k_2 \approx \exp\{2\hat{K}_1 x_3\} \iint_{\vec{k}} E(k_1,k_2)\mathrm{d}k_1\mathrm{d}k_2 ,$$

$$\iint_{\vec{k}} \omega^2 K^2 E(k_1,k_2)\exp\{2Kx_3\}\mathrm{d}k_1\mathrm{d}k_2 \approx \hat{\omega}^2\hat{K}_2^2 \exp\{2\hat{K}_2 x_3\} \iint_{\vec{k}} E(k_1,k_2)\mathrm{d}k_1\mathrm{d}k_2 ,$$

$$\iint_{\vec{k}} \frac{1}{2K+2\hat{K}_1+\hat{K}_2}\omega^2 K^2 E(k_1,k_2)\mathrm{d}k_1\mathrm{d}k_2 \approx \frac{1}{5\hat{K}_3} \iint_{\vec{k}} \omega^2 K^2 E(k_1,k_2)\mathrm{d}k_1\mathrm{d}k_2 .$$

Here we assume that $\hat{K}_1 \approx \hat{K}_2 \approx \hat{K}_3 \approx \hat{K}$ approximately. After some algebraic procedures, Eq. (B5) is reduced to

$$\left\langle \frac{\overline{k}^2}{\pi^2\overline{\varepsilon}} \right\rangle_{\mathrm{SM}} \approx \sqrt{\frac{7}{2}}\hat{\omega}\hat{K} \left(\iint_{\vec{k}} E(k_1,k_2)\mathrm{d}k_1\mathrm{d}k_2 \right)^{3/2} \exp\{3\hat{K}x_3\} \tag{B6}$$

which is Eq. (14) in Section 2.1. And by using the above unified $\hat{\omega}, \hat{K}$ and employing Eq. (B6), Eq. (11) in Section 2.1 can be derived as

$$S_{\mathrm{tid}} \approx -\frac{2\sqrt{14}}{5}\alpha_{\mathrm{wt}} K^3 \hat{\omega} \left(\iint_{\vec{k}} E(k_1,k_2)\mathrm{d}k_1\mathrm{d}k_2 \right)^{3/2} E(k_1,k_2) \tag{B7}$$

which is Eq. (15) in Section 2.1 for our further convenient numerical applications.

For monochromatic non-breaking waves, the derivation processes are similar as above. For deep water depth, we have

$$\left\langle \overline{l}_{\mathrm{D}}^2 \right\rangle_{\mathrm{SM}} \approx \frac{1}{2}A^2 \exp(2Kx_3) .$$

$$\left\langle \frac{\partial u_{\mathrm{SM}i}}{\partial x_j}\frac{\partial u_{\mathrm{SM}i}}{\partial x_j} \right\rangle_{\mathrm{SM}} = 2A^2\omega^2 K^2 \exp(2Kx_3) .$$

and

$$\left\langle \frac{\overline{k}^2}{\pi^2\overline{\varepsilon}} \right\rangle_{\mathrm{SM}} = \frac{\sqrt{7}}{4}A^3\omega K \exp\{3Kx_3\} .$$

By employing Eq. (B1), the TKE dissipation rate $\varepsilon_{\mathrm{dis}}$ can be derived as

$$\varepsilon_{\mathrm{dis}} \approx \alpha_{\mathrm{wt}} \frac{7}{8}\left\langle \frac{\overline{k}^2}{\pi^2\overline{\varepsilon}} \right\rangle_{\mathrm{SM}} \left\langle \left(\frac{\partial u_{\mathrm{SM}i}}{\partial x_j} \right)^2 \right\rangle_{\mathrm{SM}} = \frac{7\sqrt{7}}{16}\alpha_{\mathrm{wt}} A^5 \omega^3 K^3 \exp\{5Kx_3\} \tag{B8}$$

which is Eq. (19) in Section 2.1.

Appendix C

Brief derivations of Eqs. (24-27)

Assuming that the surface elevation is Gaussian and stationary and breaking occurs wherever the vertical acceleration of the surface exceeds the dynamic criterion (Longuet-Higgins, 1969; Yuan et al., 1986), the surface limited by breaking can be expressed by the Heaviside unit step function, and the postbreaking wave spectrum, via the complicated 0-1st order asymptotic expansions of the Fourier-domain covariance of surface elevation, can be formulated as Eq. (24) in Section 2.2 (Yuan et al., 1986; Hua and Yuan, 1992; Yuan et al., 1993):

$$\alpha_{\mathrm{b}} = \left[1 - 4(2\pi)^{-1/2} \frac{\rho\omega^2\mu_0^{1/2}}{g} \exp(-\frac{\rho^2}{8}\frac{g^2}{\mu_0\omega_{\mathrm{z}}^4})\right]^2 \tag{C1}$$

where $\omega_{\mathrm{z}} = (\frac{\mu_2}{\mu_0})^{1/2}$ denotes the mean zero-crossing wave frequency. Eq. (C1) can be expressed as

$$\alpha_{\mathrm{b}} = 1 - 8(2\pi)^{-1/2} \frac{\rho\omega^2\mu_0^{1/2}}{g} \exp(-\frac{\rho^2}{8}\frac{g^2}{\mu_0\omega_{\mathrm{z}}^4}) + \left[4(2\pi)^{-1/2} \frac{\rho\omega^2\mu_0^{1/2}}{g} \exp(-\frac{\rho^2}{8}\frac{g^2}{\mu_0\omega_{\mathrm{z}}^4})\right]^2 \tag{C2}$$

The third term on the right-hand side is a higher-order term compared to the second term, because the ratio of the two $r \sim \frac{\rho\omega^2\mu_0^{1/2}}{g} \sim \rho K\mu_0^{1/2} \sim \rho(AK)$, where $\rho^2 = 1 - \varepsilon_{\mathrm{sp}}^2$, $\varepsilon_{\mathrm{sp}}$ denotes the spectrum width parameter and (AK) denotes the wave steepness. Then the third term is negligible, so the ratio of total energy loss due to wave-breaking is given by

$$r_{\mathrm{b}} = \frac{\iint_{\vec{k}} E(k_1,k_2)\mathrm{d}k_1\mathrm{d}k_2 - \iint_{\vec{k}} E_b(k_1,k_2)\mathrm{d}k_1\mathrm{d}k_2}{\iint_{\vec{k}} E(k_1,k_2)\mathrm{d}k_1\mathrm{d}k_2} \approx 8(2\pi)^{-1/2} \frac{\rho\bar{\omega}^2\mu_0^{1/2}}{g} \exp(-\frac{\rho^2}{8}\frac{g^2}{\mu_0\omega_{\mathrm{z}}^4}) \tag{C3}$$

which is Eq. (25) in Section 2.2.

Yuan et al. (2009) incorporated the breaking surface elevation and the breaking criterion, then derived the breaking kinetic and potential energy loss which add up to deduce the breaking mechanical energy loss. The mechanical energy loss per unit time per unit sea surface area is formulated as

$$E_t = \frac{\rho_0 g\mu_0\mu_4^{1/2}}{2\pi\,\mu_2^{1/2}} \rho^2 \left[L\int_{-\infty}^{-L} \exp\left\{-\frac{1}{2}Z^2\right\}dZ + \exp\left\{-\frac{\rho^2}{8}\frac{g^2}{\mu_0\omega_{\mathrm{z}}^4}\right\}\right] \tag{C4}$$

(Here a slight correction is made to remove the coefficient $\sqrt{2}$ in the denominator in Eq. (54) of Yuan et al. (2009), this minor issue was introduced inadvertently in their Eq. (39) in which the coefficient 4 in the denominator is to be replaced with $2\sqrt{2}$.) Considering the appropriate time scale $T_{\mathrm{b}} = 2\pi(\frac{\mu_2}{\mu_4})^{1/2}$ associated with the loss of energy by wave breaking (Yuan et al., 1993; Donelan and Yuan ,1994), the mechanical energy loss per unit sea surface area is given

by

$$\tilde{E} = T_{\mathrm{b}} E_t = \rho_0 g \mu_0 \rho^2 \left[L \int_{-\infty}^{-L} \exp\left\{ -\frac{1}{2} Z^2 \right\} dZ + \exp\left\{ -\frac{\rho^2}{8} \frac{g^2}{\mu_0 \omega_{\mathrm{z}}^4} \right\} \right] \tag{C5}$$

In the neighborhood of wave crests $\mu_0 \bar{\omega}^2 \sim \frac{1}{2} c_0^2$, where $\bar{\omega}$ is the mean wave frequency, c_0 is the characteristic wave speed with $c_0^2 = g^2 \frac{\mu_0^{1/2}}{\mu_4^{1/2}} \rho$ (Yuan et al., 2009), so $\frac{\bar{\omega}^2 \mu_0^{1/2}}{g} = \frac{\bar{\omega}^2 \mu_0}{g \mu_0^{1/2}} \sim \frac{c_0^2}{2 g \mu_0^{1/2}} = \frac{g \mu_2}{2 \mu_0^{1/2} \mu_4}$. Then

$$\begin{aligned}
\tilde{E} &= \rho_0 g \mu_0 \frac{\mu_2}{\mu_0^{1/2} \mu_4^{1/2}} \rho \left[L \int_{-\infty}^{-L} \exp\left\{ -\frac{1}{2} Z^2 \right\} dZ + \exp\left\{ -\frac{\rho^2}{8} \frac{g^2}{\mu_0 \omega_{\mathrm{z}}^4} \right\} \right] \\
&= \rho_0 g \mu_0 \frac{g \mu_2}{2 \mu_0^{1/2} \mu_4} \rho \frac{\mu_4^{1/2}}{g/2} \left[L \int_{-\infty}^{-L} \exp\left\{ -\frac{1}{2} Z^2 \right\} dZ + \exp\left\{ -\frac{\rho^2}{8} \frac{g^2}{\mu_0 \omega_{\mathrm{z}}^4} \right\} \right] \\
&= \rho_0 g \mu_0 \frac{g \mu_2}{2 \mu_0^{1/2} \mu_4} \rho \frac{1}{L} \left[L \int_{-\infty}^{-L} \exp\left\{ -\frac{1}{2} Z^2 \right\} dZ + \mathrm{e} \exp\left\{ -\frac{\rho^2}{8} \frac{g^2}{\mu_0 \omega_{\mathrm{z}}^4} \right\} \right] \\
&\sim \rho_0 g \iint_{\vec{k}} \frac{\bar{\omega}^2 \mu_0^{1/2}}{g} \rho \frac{1}{L} \left[L \int_{-\infty}^{-L} \exp\left\{ -\frac{1}{2} Z^2 \right\} dZ + \exp\left\{ -\frac{\rho^2}{8} \frac{g^2}{\mu_0 \omega_{\mathrm{z}}^4} \right\} \right] E(k_1, k_2) \mathrm{d}k_1 \mathrm{d}k_2 \\
&\sim \rho_0 g \iint_{\vec{k}} \frac{\omega^2 \mu_0^{1/2}}{g} \rho \frac{1}{L} \left[L \int_{-\infty}^{-L} \exp\left\{ -\frac{1}{2} Z^2 \right\} dZ + \exp\left\{ -\frac{\rho^2}{8} \frac{g^2}{\mu_0 \omega_{\mathrm{z}}^4} \right\} \right] E(k_1, k_2) \mathrm{d}k_1 \mathrm{d}k_2
\end{aligned} \tag{C6}$$

In the final step of the above manipulations, for the spectral wave fields, the mean wave frequency $\bar{\omega}$ should be replaced by ω to depict the localized wave breaking. Then the attenuation coefficient in the wavenumber space is formulated as:

$$\alpha_{\mathrm{b}}' = 1 - \rho \frac{\omega^2 \mu_0^{1/2}}{g} \frac{1}{L} \left[L \int_{-\infty}^{-L} \exp\left\{ -\frac{1}{2} Z^2 \right\} dZ + \exp\left\{ -\frac{\rho^2}{8} \frac{g^2}{\mu_0 \omega_{\mathrm{z}}^4} \right\} \right] \tag{C7}$$

which is Eq. (26) in Section 2.2.

Let $\theta \equiv L \int_{-\infty}^{-L} \exp\left\{ -\frac{1}{2} Z^2 \right\} \mathrm{d}Z \Big/ \exp\left\{ -\frac{\rho^2}{8} \frac{g^2}{\mu_0 \omega_{\mathrm{z}}^4} \right\}$ represents the ratio of the kinetic energy loss to the potential one due to wave-breaking with a range of 3 to 30 (Yuan et al., 2009; Wang et al., 2017, 2018), Eq. (C7) can be rewritten as

$$\alpha_{\mathrm{b}}' = 1 - \rho \frac{\omega^2 \mu_0^{1/2}}{g} \frac{1 + \theta}{L} \exp\left\{ -\frac{\rho^2}{8} \frac{g^2}{\mu_0 \omega_{\mathrm{z}}^4} \right\} \tag{C8}$$

which is Eq. (27) in Section 2.2.

Key references

Baumert, H. Z., Simpson, J. H., and Sündermann, J. (Eds.): Marine turbulence: theories, observations, and models, Cambridge University Press, Cambridge, UK, 630pp., ISBN 978-0-521-15372-0, 2005.

Hua F., and Yuan, Y.: Theoretical study of breaking wave spectrum and its application, Sci. China Ser. B, 9, 958-965, 1992.

Longuet-Higgins, M. S.: On wave breaking and equilibrium spectrum of wind, Proc. Roy. Soc. London, 310A, 151-159, 1969.

Wang, H., Yang, Y., Dong, C., Su, T., Sun, B., and Zou, B.: Validation of an improved statistical theory for sea surface whitecap coverage using satellite remote sensing data, Sensors, 18, 3306, https://doi.org/10.3390/s18103306, 2018.

Wang, H., Yang, Y., Sun, B., and Shi, Y.: Improvements to the statistical theoretical model for wave breaking based on the ratio of breaking wave kinetic and potential energy, Sci. China Earth Sci., 60(1), 180-187, https://doi.org/10.1007/s11430-016-0053-3, 2017.

Yuan, Y., Han, L., Hua, F., Zhang, S., Qiao, F., Yang, Y., and Xia, C.: The statistical theory of breaking entrainment depth and surface whitecap coverage of real sea waves, J. Phys. Oceanogr., 39, 143-161, https://doi.org/10.1175/2008JPO3944.1, 2009.

Yuan, Y., Hua, F., Pan, Z., and Sun, L.: Dissipation source function and improvement of LAGFD-WAM numerical wave model, Oceanol. Limnol. Sin., 24(4), 367-376, 1993.

Yuan, Y., Qiao, F., Hua, F., and Wang, Z.: The development of a coastal circulation numerical model: I. Wave-induced mixing and wave-current interaction, J. Hydrodyn. Ser. A, 14, 1-8, 1999.

Yuan, Y., Qiao, F., Yin, X., and Han, L.: Analytical estimation of mixing coefficient induced by surface wave-generated turbulence based on the equilibrium solution of the second-order turbulence closure model, Sci. China Earth Sci., 56, 71-80, https://doi.org/10.1007/s11430-012-4517-x , 2013.

Yuan, Y., Tung, C. C., and Huang, N. E.: Statistical characteristics of breaking waves, in: Wave Dynamics and Radio Probing of the Ocean Surface, edited by: Phillips, O. M., and Hasselmann, K., Plenum Press, New York, 265-272, ISBN 0-306-41992-0, 1986.

3.3.2 *Clarification of numerical constants and closure assumptions*

The manuscript introduces specific numerical coefficients (e.g. 7, 7/8, and others) that originate from minimization principles or closure assumptions. Their physical or mathematical origin should be documented more clearly. For example, it would help to explain more about the constant 7 appearing in the mixing-length formulation, including a brief explanation of the assumptions and limitations. Same with the 7/8 coefficient. Sensitivity to these constants should be briefly discussed.

These numerical coefficients were obtained via the minimization relation for the equilibrium solutions of the k - ε type eddy viscosity model (Yuan et al., 2013), i.e, $\overline{\varepsilon} \approx \frac{7}{8}\frac{\overline{k}^2}{\pi^2\overline{\varepsilon}}\left(\frac{\partial u_{\mathrm{SM}i}}{\partial x_j}\right)^2$. The approximate coefficient 7/8 indicates that the shear instability generation of surface waves is the dominant source of the turbulence in the upper ocean. Based on the k - ε type eddy viscosity model, Zhuang et al. (2021) further examined the effect of the buoyancy flux on the turbulent mixing via comparisons of the calculated TKE dissipation rates with cruise observations at 12 stations, and revealed that the buoyancy flux slightly suppresses the enhanced vertical mixing induced by non-breaking wave-generated turbulence. This is consistent with the previous results that at a steady state the buoyancy flux term will not exceed 13%-17% of the whole TKE dissipation rate (Ferrari et al., 2016; Gibson, 1981; Osborn, 1980). In numerical modeling, these constants, via Eq. (15), are incorporated into the coefficient α_{wt} and its sensitivity is evaluated in the simple duration-limited growth and decay experiments in Section 3, where $\alpha_{\mathrm{wt}} = 0.05,\ 0.06$ or $\alpha_{\mathrm{wt}} = 0.15$ for the linear or quasi-linear growth parameterizations of wind input source function.

Babanin (2011) interpreted that, if averaged over the wave period, the estimates of $\varepsilon_{\mathrm{dis}}$ have to be divided at least by a factor of 10 and perhaps more, and in our numerical modeling, the coefficient α_{wt} should be tuned to 0.02 - 0.2. Wang et al. (2024) also evaluated its sensitivity by comparing to the Jason-3 satellite altimeter observation data and four non-nearshore NDBC buoys data.

Key references

Babanin, A.V.(Eds.): Breaking and Dissipation of Ocean Surface Waves, Cambridge University Press, Cambridge, UK, 480pp., ISBN 978-1-107-00158-9, https://doi.org/10.1017/CBO9780511736162, 2011.

Ferrari, R., Mashayek, A., McDougall, T. J., Nikurashin, M., and Campin, J.-M.: Turning ocean mixing upside down. Journal of Physical Oceanography, 46(7), 2239-2261. https://doi.org/10.1175/jpo-d-15-0244.1, 2016.

Gibson, C. H.: Buoyancy effects in turbulent mixing: Sampling turbulence in the stratified ocean. AIAA Journal, 19(11), 1394-1400, https://doi.org/10.2514/3.60076, 1981.

Osborn, T. R.: Estimates of the local rate of vertical diffusion from dissipation measurements. Journal of Physical Oceanography, 10, 83-89, https://doi.org/10.1175/1520-0485(1980)010<0083:eotlro>2.0.co;2, 1980.

Wang, F., Yang, Y., Yin, X., Jiang, X., and Sun, M.: Improving wave modeling performance by incorporating wave-generated turbulence dissipation and improved post-breaking spectrum, Ocean Modell., 188 (2024) 102311, https://doi.org/10.1016/j.ocemod.2023.102311, 2024.

Yuan, Y., Qiao, F., Yin, X., and Han, L.: Analytical estimation of mixing coefficient induced by

surface wave-generated turbulence based on the equilibrium solution of the second-order turbulence closure model, Sci. China Earth Sci., 56, 71-80, https://doi.org/10.1007/s11430-012-4517-x , 2013.

Zhuang, Z., Yuan, Y., Zheng, Q., Zhou, C., Zhao, X., and Zhang, T.: Effects of buoyancy flux on upper-ocean turbulent mixing generated by nonbreaking surface waves observed in the South China Sea. Journal of Geophysical Research: Oceans, 126, e2020JC016816, https://doi.org/10.1029/2020JC016816, 2021.

3.3.3 *Physical assumptions should be more explicitly addressed*

The work is strong but theory relies heavily on assumptions that must be articulated and justified. Including the Quasi-equilibrium between production and dissipation in wave-generated turbulence; Applicability of linear wave theory to turbulence generation; the scaling assumptions connecting orbital velocity gradients to turbulent production; and Statistical assumptions underlying the breaking-wave attenuation model. The work would benefit from a short section discussing the validity and limitations of these assumptions.

We thank for the reviewer's constructive suggestions and a supplemental paragraph was appended to the end of Section 4 to address these physical assumptions as follows:

Finally, some limitations of underlying assumptions in our theoretical arguments require further discussions. In the k - ε type eddy viscosity model of wave-generated turbulence, the turbulence timescale is assumed to be shorter than waves. Therefore, the interaction of turbulence at other scales with ocean waves, which also accounts for a significant fraction of the energy losses of the wave field, is not included in our practical numerical wave model. The quasi-equilibrium assumption of wave-generated turbulence poses the problem of an undetermined coefficient, which needs further elaborations especially essential precise measurements. The linear non-breaking wave theory applied to construct analytical solutions for the turbulence generation is an acceptable assumption in the general case of weakly nonlinear situations, and the scale estimation via the shear instability of wave orbital motions only represents a major portion of the turbulent production in the upper ocean. As stated by Yuan et al. (2009), since the wave spectrum in real-world scenarios is not actually narrow, the breaking wave statistical method under a narrow spectrum assumption is not precise enough to estimate the attenuation coefficient for the postbreaking wave spectrum.

Key references

Yuan, Y., Han, L., Hua, F., Zhang, S., Qiao, F., Yang, Y., and Xia, C.: The statistical theory of breaking entrainment depth and surface whitecap coverage of real sea waves, J. Phys. Oceanogr., 39, 143-161, https://doi.org/10.1175/2008JPO3944.1, 2009.

3.3.4 *Notation consistency and clarity*

The work relies heavily on mathematical expressions. Nevertheless, the notation usage is occasionally inconsistent or overly dense. For example: The distinction between k and K for wavenumber components vs. magnitude should be standardized. There are inconsistencies with vertical coordinate definitions that vary between sections. It would be beneficial to define every variable used and keep them consistent. Also, the use of overbars, hats, and primes for averaged quantities should be clearly defined and applied uniformly. Maybe a notation table could improve readability.

We thank the reviewer's constructive suggestions. A table for variable notation was supplemented in Appendix D of the revised manuscript (see below).

Appendix D

Variable notation

As this study relies heavily on mathematical expressions, a list of symbols is provided in Table D1.

No.	Symbol	Notation
1	$x_i, i = 1, 2, 3$	Rectangular co-ordinate variables
2	$u_{\mathrm{SM}i}, i = 1, 2, 3$	Wave velocity components
3	$u_{\mathrm{w}0}$	Wave orbital velocity at sea surface
4	u_*	Friction velocity
5	τ_{w}, τ	Wave-induced stress and total stress
6	$\hat{N}_i, i = 1, 2, 3$	Brunt–Väisälä frequency components
7	k, ε	Turbulent kinetic energy (TKE) and TKE dissipation rate
8	$\overline{k}$, $\overline{\varepsilon}$, and $\overline{l_D}$	Equilibrium variables of TKE and TKE dissipation rate, and mixing length
9	e_{tid}, $\varepsilon_{\mathrm{dis}}$	Unit volume wave energy dissipation rate and TKE dissipation rate induced by wave-generated turbulence
10	ω	Wave radian frequency
11	A	Wave amplitude
12	$\vec{\boldsymbol{k}}$, k_1, k_2 and K	Wavenumber vector and wavenumber components with $\vec{\boldsymbol{k}} = (k_1, k_2)$, wavenumber magnitude with $K = \sqrt{k_1^2 + k_2^2}$
13	C	Phase velocity with $C = \frac{\omega}{K}$
14	$\hat{K}_1, \hat{K}_2, \hat{K}_3, \hat{K}$, and $\hat{\omega}$	Characteristic wavenumbers and frequency

15	$E(k_1,k_2)$	Wavenumber spectrum
16	μ_i	*i-th* order moment of the wave spectrum
17	ε_{sp}, ρ	Spectrum width parameter and parameter with $\rho=\sqrt{1-\varepsilon_{sp}^2}$
18	T_b, ω_b, T_z and ω_z	Mean period and mean frequency of wave maxima with $\omega_b=\frac{2\pi}{T_b}$, mean zero-crossing wave period and wave frequency
19	$\bar{\omega}$ and c_0	Mean wave frequency and characteristic wave speed with $c_0=\sqrt{g^2\frac{\mu_0^{1/2}}{\mu_4^{1/2}}\rho}$ associated with breaking wave crests
20	$\hat{\omega}$	Mean wave frequency with $\hat{\omega}=\left(\mu_{-1}/\mu_0\right)^{-1}$

Table D1. Variable notation

3.3.5 *Validation of the model*

While the comparison with laboratory data is promising, it is currently limited in scope to strengthen the validation. A short description of the experimental datasets used could help, and a discussion of the uncertainty in both measurements and model predictions. A comparison with existing dissipation parameterizations could also strengthen the work (e.g. WAM/WW3 whitecapping formulas) and the sensitivity to model parameters such as α_{wt}. Including a short description of the model employed would further aid reader understanding.

We agree the reviewer' point that the scope limitation for model validation is the weakest part of the manuscript. As per the reviewer's suggestions, A short description for the two sets of experimental data was supplemented before verification of the modeled TKE dissipation rate ε_{dis} in Section 2.1 as follows:

> Two sets of experimental data are selected to verify the modeled TKE dissipation rate ε_{dis} below. For the first set of laboratory measurements, in order to avoid ambiguity due to wind-caused shear stresses and other dynamic mechanisms, a simple setup for unforced mechanically generated monochromatic wave trains was realized. For the second set of laboratory measurements, wave-induced turbulence with regard to the wind wave, swell and mixed wave conditions, as well as the decreasing tendency of the TKE dissipation rate with layer depth, was conducted for joint comparisons.

A supplemental paragraph to address the uncertainty in both measurements and model predictions was appended to the end of Section 2.1 as follows:

The turbulence production is attributed to the wave-generation conditions. The turbulence observed in the first set of measurement data is directly generated by the waves themselves. While in the second set of measurement data, turbulence generation may be governed by complex dynamical mechanisms, and only the wave-induced turbulence is considered here.

The ‘‘observed’’ TKE dissipation rates $\varepsilon_{\mathrm{dis}}$ in both sets of measurement data correspond to the instantaneous state when turbulence occurs, and in the above comparative experiments we set the quasi-equilibrium coefficient $\alpha_{\mathrm{wt}} = 1.0$ in our model for the estimates of $\varepsilon_{\mathrm{dis}}$. This introduces uncertainty with regard to phase averaging in practical numerical modeling, which is discussed further in Section 4.

The in-lake site measurement to obtain the valuable breaking spectra and the nonbreaking spectra for the spectral difference was described in Section 2.2. The deficiencies of our improved statistical model were discussed and supplemented in the revised manuscript as follows:

The calculated attenuation coefficients correspond to this tendency, which yields valuable insights of the physics of dominant breaking, but the statistical approach is less well-suited for simulating the rapid transient regime of wave breaking as well as for the higher frequency in the equilibrium range.

In order to evaluate the new dissipation formulations due to wave-generated turbulence and wave-breaking, which are focal points of the present study, the scaling behavior for the duration-limited growth and decay is demonstrated and interpreted in section 3. Numerical experiments were performed and model results were compared to the original MASNUM wave model and WAM wave model (Janssen et al., 1994). Figures 7-9 show the new model results comparing to those existing dissipation parameterizations, while other source functions S_{nl}, S_{bo} and S_{cu} are not changed. As per the reviewer’s suggestions, a brief description of the models employing the existing dissipation parameterizations was supplemented in the revised manuscript as follows:

The wave-breaking dissipation source function in the original MASNUM wave model is given as

$$S_{\mathrm{ds}} = -d_1 \bar{\omega} \left(\frac{\omega}{\bar{\omega}} \right)^2 \left(\frac{\hat{\alpha}}{\hat{\alpha}_{\mathrm{PM}}} \right)^{1/2} \exp\left\{ -d_2 (1 - \varepsilon_{\mathrm{sp}}^2) \frac{\hat{\alpha}_{\mathrm{PM}}}{\hat{\alpha}} \right\} E(k_1, k_2)$$

where $\bar{\omega} = \left(\mu_{-1} / \mu_0 \right)^{-1}$, $\hat{\alpha} = \mu_0 \bar{\omega}^4 g^{-2}$, $\hat{\alpha}_{\mathrm{PM}}$ is the value of $\hat{\alpha}$ for a PM spectrum ($\hat{\alpha}_{\mathrm{PM}} = 3.02 \times 10^{-3}$). Two critical coefficients d_1 and d_2 ($d_1 = 1.32 \times 10^{-4}$, $d_2 = 2.61$) were retrieved through fitting algorithm with the dimensional expression proposed by Komen et al. (1984). The corresponding dissipation term in the WAM-Cycle models is given as.

$$S_{\mathrm{ds}} = -C_{\mathrm{ds}} \bar{\omega} \left(\frac{\omega}{\bar{\omega}} \right)^2 \left(\frac{\hat{\alpha}}{\hat{\alpha}_{\mathrm{PM}}} \right)^2 E(k_1, k_2)$$

where C_{ds} is a constant ($C_{\mathrm{ds}} = 2.36 \times 10^{-5}$).

In numerical modeling in Section 3, the sensitivity of the coefficient α_{wt} is evaluated in the duration-limited growth and decay experiments, where $\alpha_{wt} = 0.05,\ 0.06$ or $\alpha_{wt} = 0.15$ for the linear or quasi-linear growth parameterizations of wind input source function. Babanin (2011) interpreted that, if averaged over the wave period, the estimates of ε_{dis} have to be divided at least by a factor of 10 and perhaps more. Based on the new model for global hindcast and forecast, Wang et al. (2024) also evaluated the sensitivity of α_{wt} by comparing to the Jason-3 satellite altimeter observation data and four non-nearshore NDBC buoys data, an adjusted coefficient $\alpha_{wt} = 0.0245$ was derived by fitting the modeled wave height against observations. Collectively, our sensitivity analysis suggests that the coefficient α_{wt} should be in the ranges of 0.02 - 0.2. In our numerical experiments, the constant α_{wt} is chosen as a tuned coefficient. Physically, it is certainly not constant at any instant *t* in real-world scenarios, which is discussed further in Section 4.

Key references

Janssen, P. A. E. M., Giinther, H., Hasselmann, S., Hasselmann, K., Komen, G. J., and Zambresky, L.: Simple tests, in: Dynamics and Modelling of Ocean Waves, edited by: Komen, G. J., Cavaleri, L., Donelan, M.,Hasselmann, K., Hasselmann, S., and Janssen, P. A. E. M., Cambridge University Press, Cambridge, UK, 244-257, ISBN 0-521-47047-1, 1994.

The WAVEWATCH III® Development Group (WW3DG): User manual and system documentation of WAVEWATCH III® version 6.07, Tech. Note 333, NOAA/NWS/NCEP/MMAB, College Park, MD, USA, 465 pp. +Appendices, 2019.

WAMDI Group: The WAM model-A third generation ocean wave prediction model, J. Phys. Oceanogr., 18, 1775-1810, 1988.

Wang, F., Yang, Y., Yin, X., Jiang, X., and Sun, M.: Improving wave modeling performance by incorporating wave-generated turbulence dissipation and improved post-breaking spectrum, Ocean Modell., 188 (2024) 102311, https://doi.org/10.1016/j.ocemod.2023.102311, 2024.

Yuan, Y., Hua, F., Pan, Z., and Sun, L.: LAGFD-WAM numerical wave model-I. Basic physical model, Acta Oceanol. Sin., 10(4), 483-488, 1991.